
Learning the Feedback Connections from V1 to LGN via Information Maximization

Reza Eghbali*
Berkeley Institute for Data Science
University of California, Berkeley
Berkeley, CA 94720
eghbali@berkeley.edu

Fritz Sommer
Helen Wills Neuroscience Institute
University of California, Berkeley
Berkeley, CA 94720
fsommer@berkeley.edu

S. Murray Sherman
Department of Neurobiology
University of Chicago
Chicago, IL 60637
ssherman@uchicago.edu

Abstract

1 The lateral geniculate nucleus (LGN) relay cells act as a gateway for transmitting
2 visual information from retina to the primary visual cortex (V1). The activities
3 of thalamic relay cells are modulated by feedback connections emanating from
4 layer 6 of V1. While the receptive field (RF) properties of these early parts of
5 the visual system are relatively well understood, the function, computational role,
6 and details of the feedback network from V1 to LGN are not. Computational
7 models of efficient coding have been successful in deriving RF properties of
8 retinal ganglion and V1 simple cells by optimizing the Shannon information.
9 Further, previous experimental results have suggested that the feedback increases
10 the Shannon information. Motivated by this earlier work, we try to understand
11 the function of the feedback as optimizing the feedforward information to cortex.
12 We build a model that learns feedback weights by maximizing the feedforward
13 Shannon information on naturalistic stimuli. Our model predicts the strength
14 and sign of feedback from a V1 cell to all ON- and OFF-center LGN relay cells
15 that are within or surrounding the V1 cell RF. We find a highly specific pattern
16 of influence on ON and OFF-center LGN overlapping the V1 RF depending on
17 whether they overlapped the ON or OFF zone of the V1 RF. In addition, we find
18 general inhibitory feedback in the further surround, which sharpens the RFs and
19 increases surround suppression in LGN relay cells. This is consistent with results
20 of recent experiments exploring the impact of feedback on stimuli integration.

21 1 Introduction

22 The lateral geniculate nucleus (LGN) acts as a relay of information from the retina to the primary
23 visual cortex (V1). This information flow is modulated by top-down feedback from layer 6 of V1 to
24 LGN. While the input from the retina is the driver input for the LGN relay cells, the feedback is the
25 modulating input for these cells [29]. There is a large body of experimental work on the functionality
26 of the feedback pathway from V1 to LGN. It has been observed that this feedback can play an

*eghbali@uw.edu, reza.eghbali@ucsf.edu

27 important role in burst vs tonic firing of relay cells [28], increase the timing precision [1, 16], and
28 affect the spatial specificity of LGN relay cells [12, 19].

29 Anatomical evidence indicates that the corticogeniculate feedback monosynaptically excites an LGN
30 relay cell and disynaptically inhibits it through the thalamic reticular nucleus or the local inhibitory
31 neuron in LGN [10]. Thus, the feedback can have both signs, it can be excitatory or inhibitory.
32 Moreover, the experiments conducted on primates suggest that this feedback is pathway-specific, with
33 parvocellular, magnocellular, and koniocellular LGN cells each receiving input from distinct classes
34 of layer 6 cell [8]. In dual recordings of V1 and LGN, Tsumoto et al. observed mostly excitatory
35 feedback if the V1 and LGN RFs were within 2.4° and inhibitory impact beyond that up to 3.1° [30].

36 These types of experimental findings have inspired the modeling of the feedback as an excitatory-
37 center inhibitory-surround network [14]. A model proposed by Mobarhan et al., in which the feedback
38 center and surround effects were fitted to experimental data on spatial integration in the dorsal LGN
39 [24] also showed an excitatory-center inhibitory-surround. Dual recording experiments conducted
40 by Want et al. [32, 33] suggest an even more specific pattern of connections. Specifically, in [32],
41 the authors observe that LGN cells were significantly more likely to be impacted by feedback, either
42 through facilitation or suppression, when their location was displaced in parallel or orthogonal
43 directions relative to the preferred orientation of the V1 cells. In [33], by measuring the burst-to-tonic
44 ratio in LGN, they established a phase-reversed pattern of connections for LGN cells that overlap the
45 V1 RF.

46 There is no shortage of existing hypotheses about the functional role of feedback from V1 to LGN,
47 probably starting with [15], who suggested the feedback could modify LGN responses iteratively to
48 help the interpretation of the input. Feedback models were designed and discussed in the context
49 of different visual tasks, such as line perception [27], visual grouping [13, 14], visual attention
50 [6, 9, 22, 25], etc.

51 Here we asked whether there could be an even simpler explanation of the feedback circuitry, the
52 adaptation of the circuit for maximizing the LGN to V1 information flow. Originating in the work of
53 [4, 2], this idea has gathered a lot of momentum. Experiments conducted by Mcclurkin et al. revealed
54 that cooling V1 in awake monkeys reduced the average stimulus-related information transmitted
55 by LGN neurons [23]. Further, principles of information maximization and efficient coding have
56 been widely successful in understanding the structure of feedforward connections in the early visual
57 system. These principles lead to normative models that learn V1-like receptive fields from natural
58 images [5, 31, 26]. Similarly, the same principles, when combined with realistic noise levels present
59 in the retina, yield models that reproduce the center-surround receptive fields of retinal ganglion cells
60 [20].

61 We designed a novel type of normative model that employs the same information objective, in a
62 circuitry with feedback. As forward connections, we use the known RF structure of LGN and cortex,
63 the feedback connections are optimized by learning during naturalistic stimulation. The learned
64 feedback weights show reciprocal excitation of LGN cells that are exciting the V1 cells, and inhibition
65 of the LGN cells that inhibit the V1 cell. These weights also show a pattern of suppression for LGN
66 cells that are retinotopically displaced relative to the V1 RF within 4 - 6 times the receptive field size.
67 Testing the impact of this learned feedback on spatial integration in LGN points to an accentuation of
68 surround suppression as a result of feedback which is also consistent with experimental results in [7].

69 2 Model

70 We use rate code models of retina, LGN, and V1 to represent the feedforward pathway from retina
71 to V1. Given a two-dimensional gray-scale input image X , the retinal output is calculated as
72 $Y_{\text{retina}}^p = f_{\text{retina}}^p(W_{\text{retina}}^p * X)$ for $p \in \{\text{ON}, \text{OFF}\}$, where $W_{\text{retina}}^{\text{ON}}$ and $W_{\text{retina}}^{\text{OFF}}$ are the ON and OFF-
73 center retinal ganglion cell linear filter weights and $*$ denotes the two-dimensional convolution
74 operator. Each linear filter has an associated rectifying nonlinearity f_{retina}^p which is applied entry-wise
75 to the two-dimensional convolution $W_{\text{retina}}^p * X$. The rectifying nonlinearity is given as

$$f(I) = \max(RI - v, 0), \quad (1)$$

76 where $R > 0$ and v are nonlinearity parameters. Note that the scaling factor R is required since
77 the linear filter weights are fixed. The ON and OFF-center filters are shown in Figure 1A. The two
78 linear filters are 27 by 27 pixel discrete approximations of a two-dimensional difference-of-Gaussians

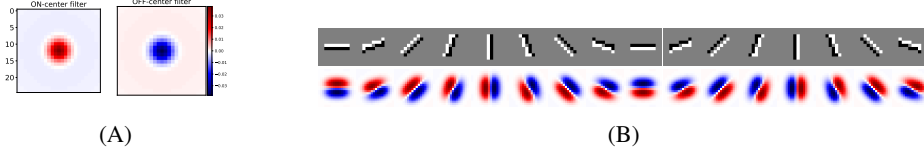


Figure 1: **Feedforward and feedback models.** A: ON and OFF Difference of Gaussian filters used in the model of retina. The filters parameters are: $(\sigma_1, \sigma_2, k) = (2, 14, 0.9)$. B: The V1 weights and the corresponding receptive fields when the weights are applied to ON and OFF-center LGN cells.

79 (DoG) filter given by $\pm \frac{1}{2\pi\sigma_1^2} e^{-(v_1^2+v_2^2)/(2\sigma_1^2)} \mp \frac{k}{2\pi\sigma_2^2} e^{-(v_1^2+v_2^2)/(2\sigma_2^2)}$. We set $\sigma_2/\sigma_1 = 7$ and $k = 0.9$
 80 which are biologically plausible based on measurements in cat retina [11]. The convolution operation
 81 has a stride (spacing between neighboring cells) of $2\sigma_1$. This spacing is chosen based on reported
 82 measurements of the retina and computational work showing that information from natural images
 83 peaks at a receptive field spacing of $\sim 2\sigma_1$ [3].

84 In our model each LGN relay cell is driven by a single RGC and the LGN output is $Y_{\text{LGN}}^p =$
 85 $f_{\text{LGN}}^p(Y_{\text{retina}}^p)$ for $p \in \{\text{ON}, \text{OFF}\}$, where f_{LGN}^p are rectifying nonlinearities of type given in (1). The
 86 LGN output then serves as input to V1. To create the V1 output, we form Hubel and Wiesel V1 simple
 87 cells [17] by assigning equal positive weights to 8 ON LGN and 8 OFF-center LGN cells along 8
 88 different directions. These 8 filters alongside their phased-reversed version form the V1 filterbank of
 89 size 16 (see Figure 1B). The V1 output is given by $Y_{\text{V1}}^k = f_{\text{V1}}^k(\sum_{p \in \{\text{ON}, \text{OFF}\}} W_{\text{V1}}^{k,p} * Y_{\text{LGN}}^p)$ for $k \in$
 90 $\{0, 1, \dots, 15\}$, where f_{V1}^k is applied entry-wise to the output of the convolution.

91 2.1 Feedback model

92 The majority of the deriving axons from LGN relay cells target cells in layer 4C of the cortex, while
 93 the feedback to the LGN emanates from layer 6. Hence a complete model of the feedback should
 94 include the mechanisms that give rise to layer 6 cells' receptive fields requiring access to many
 95 unknown parameters related to the micro-circuitry in a V1 column. To avoid these complications, we
 96 model the feedback as direct feedback from the same V1 cells that are being driven by LGN.

97 We allow a V1 cell to feedback on LGN relay cells directly overlapping the V1 cell RF or within a
 98 retinotopic neighborhood of the V1 cell RF. Associated with each one of the 16 V1 filter types, there
 99 are two sets of two-dimensional feedback weights which determine the feedback impact on ON and
 100 OFF-center LGN cells. These weights are denoted by $W_{\text{fb}}^{k,\text{ON}}$ and $W_{\text{fb}}^{k,\text{OFF}}$ for $k \in \{0, 1, 2, \dots, 15\}$.
 101 The V1 activation after applying the feedback will be the solution to the following equation:

$$Y_{\text{V1}}^k = f_{\text{V1}}^k \left(\sum_{p \in \{\text{ON}, \text{OFF}\}} W_{\text{V1}}^{k,p} * f_{\text{LGN}}^p \left(Y_{\text{retina}}^p + \sum_{l=0}^{15} W_{\text{fb}}^{l,p} * Y_{\text{V1}}^l \right) \right) \text{ for } k \in \{0, 1, \dots, 15\}.$$

102 Figure 3A depicts a block diagram of the model. To numerically estimate Y_{V1} , we unroll this feedback
 103 loop in 3 steps, a standard technique used for recurrent neural networks.

104 3 Learning the feedback weights

105 To learn the feedback kernel and nonlinearity parameters in the feedforward model, we use an
 106 information objective. Since we are considering a noiseless channel from retina to V1, the mutual
 107 information between the input image patches and the V1 output is given by the differential entropy
 108 of the V1 output. Differential entropy increases when the firing rates are scaled up. Therefore, our
 109 optimization objective, similar to the objective used in [20], has a penalty term that penalizes the
 110 average firing rate. We calculate an upper bound on the differential entropy of a 2×2 patch of V1
 111 cells, where each location is covered by 16 types of V1 cells. Let Y_{patch} be the vectorized response
 112 vector of these 64 cells. We denote the differential entropy of Y_{patch} by $H(Y_{\text{patch}})$ and note that
 113 $H(Y_{\text{patch}}) \leq \frac{1}{2} \log \det(\Sigma_{Y_{\text{patch}}}) + \text{const.}$, where $\Sigma_{Y_{\text{patch}}}$ is the empirical covariance of Y_{patch} . We
 114 maximize a penalized version of this upper bound on the information:

$$(1 - \lambda) \log \det(\Sigma_{Y_{\text{patch}}}) - \lambda \mathbf{1}^T \bar{Y}_{\text{patch}}, \quad (2)$$

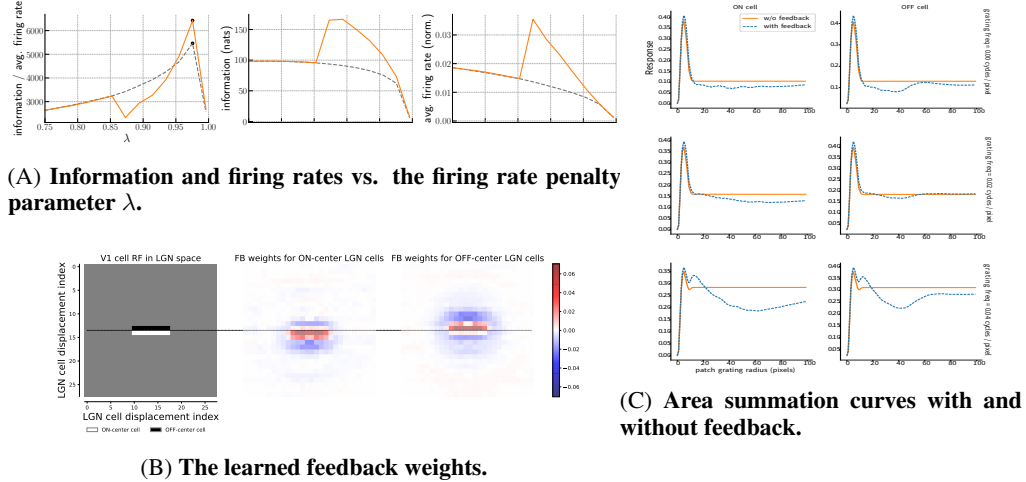


Figure 2: A The information normalized by average firing rate, information, and average firing rate of V1 as for $\lambda \in [0.75, 1)$ with and without feedback. B The learned feedback weights for $\lambda = 0.988$ which achieves the maximum information per spike. The feedback weights for ON-center (OFF-center) LGN cells determine the impact of the feedback from the V1 cell on ON-center (OFF-center) LGN cells. C The response of an ON and an OFF LGN cell as a function of the size of the patch sinusoidal grating for three different spatial frequencies with and without feedback.

115 where $\lambda \in (0, 1)$ is the firing rate penalty parameter and \bar{Y}_{patch} is the empirical mean of Y_{patch} .
 116 We perform gradient ascent on the upper bound given in (2) to find the feedback kernels and the
 117 nonlinearity parameters. The gradients are calculated using automatic differentiation available in the
 118 PyTorch library. We use step size of 10^{-4} and run the optimization for 2500 full batch iterations².
 119 The parameter λ is varied in $[0.775, 1)$. For each value of λ , we solved two optimization problems:
 120 one only over feedforward model nonlinearity parameters without any feedback, and one over both
 121 the feedback and feedforward model parameters.

122 Figure 2A shows the information, information per spike, and the average firing rate when λ ranges
 123 from 0.75 to 1. The information per spike with feedback achieves its maximum of 7154 for $\lambda = 0.988$.
 124 This is greater than the maximum achieved without feedback by approximately %14. The learned
 125 feedback weights for $\lambda = 0.988$ show a pattern of connection that is aligned with the V1 RF
 126 (Figure 2B). In other words, feedback excites the ON(OFF)-center LGN cells that overlap the
 127 ON(OFF) region of the V1 receptive field. The feedback weights have a small inhibitory impact on
 128 the phase reversed cells. Those are the ON(OFF)-center cells on the OFF(ON) regions of the V1
 129 receptive field. Another signature of the feedback pattern is a general inhibition of the LGN cells in a
 130 neighborhood of the V1 cell RF elongated in the preferred orientation of the cell. This can explain
 131 the impact of this feedback on stimuli integration, which is explored in section 3.1.

132 3.1 Impact of feedback on RF properties

133 To investigate the impact of the feedback on LGN RF properties, we computed the area summation
 134 curve for ON and OFF-center LGN cells with and without feedback. These curves are computed by
 135 measuring the peak response of the LGN cell to a windowed moving sinusoidal grating as the size of
 136 the window increases from zero to a few multiples of the LGN RF size. Figure 2C shows the area
 137 summation curves for spatial freq = 0 (light spot for ON-center cell, dark spot for OFF-center cell),
 138 0.02 and 0.04 (cycles / pixel). In all three cases, feedback increases the peak firing rate for small
 139 windows and decreases the firing rate for large window sizes. This is in agreement with experimental
 140 results in [7], which show a similar feedback effect on stimuli integration in LGN.

²The code and natural images used to produce the results of this paper are available at <https://anonymous.4open.science/r/learning-v1-lgn-feedback-9DBE>.

141 3.2 Phase-aligned vs phase-reversed

142 Our model suggests a phase-aligned feedback arrangement for the LGN cells directly overlapping
143 the V1 RF consistent with results in [7, 24]. In [33], by measuring the burst-to-tonic ratios for LGN
144 cells after feedback deactivation, the authors deduce a phase-reversed arrangement for LGN cells that
145 directly overlap the V1 cell RF. In [18], A computational model based on predictive coding has been
146 suggested to account for this. In a recent work, Lian et al propose a model of V1-LGN pathway based
147 on efficient coding that learns the feedback weights using an anti-Hebbian rule [21]. This makes
148 the feedback weights converge to the negative of feedforward weights, resulting in a phase-reversed
149 pattern. However, there is overwhelming evidence that feedback impact goes beyond the receptive
150 field of the V1 cell [30, 32]. We believe more comprehensive experiments are required to resolve
151 these conflicting results.

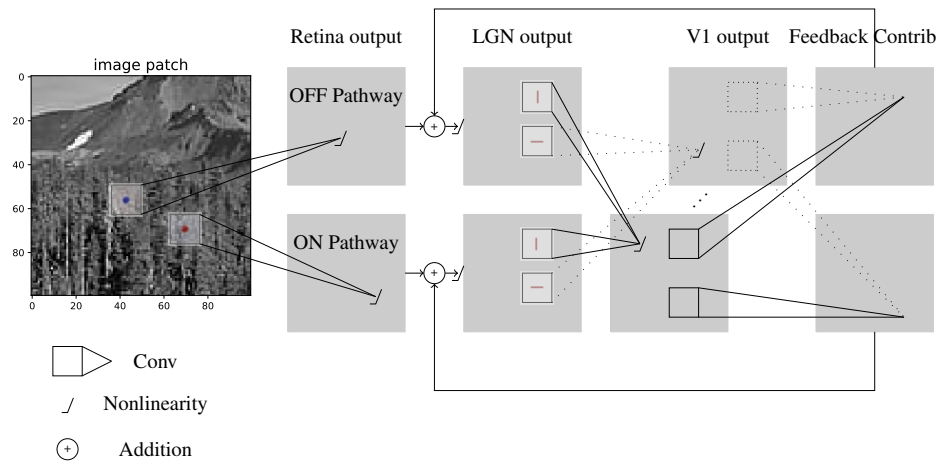
152 References

- 153 [1] I. M. Andolina, H. E. Jones, W. Wang, and A. M. Sillito. Corticothalamic feedback enhances stimulus
154 response precision in the visual system. *Proceedings of the National Academy of Sciences*, 104(5):1685–
155 1690, 2007.
- 156 [2] F. Attneave. Some informational aspects of visual perception. *Psychological review*, 61(3):183, 1954.
- 157 [3] V. Balasubramanian and P. Sterling. Receptive fields and functional architecture in the retina. *The Journal*
158 *of physiology*, 587(12):2753–2767, 2009.
- 159 [4] H. B. Barlow et al. Possible principles underlying the transformation of sensory messages. *Sensory*
160 *communication*, 1(01), 1961.
- 161 [5] A. J. Bell and T. J. Sejnowski. The "independent components" of natural scenes are edge filters. *Vision*
162 *research*, 37(23):3327–3338, 1997.
- 163 [6] J. Bickle, M. Bernstein, M. Heatley, C. Worley, and S. Stiehl. A functional hypothesis for lgn-v1-trn
164 connectivities suggested by computer simulation. *Journal of computational neuroscience*, 6(3):251–261,
165 1999.
- 166 [7] G. Born, F. A. Schneider-Soupiadis, S. Erisken, A. Vaiceliunaite, C. L. Lao, M. H. Mobarhan, M. A.
167 Spacek, G. T. Einevoll, and L. Busse. Corticothalamic feedback sculpts visual spatial integration in mouse
168 thalamus. *Nature neuroscience*, 24(12):1711–1720, 2021.
- 169 [8] F. Briggs and W. M. Usrey. Parallel processing in the corticogeniculate pathway of the macaque monkey.
170 *Neuron*, 62(1):135–146, 2009.
- 171 [9] F. Crick. Function of the thalamic reticular complex: the searchlight hypothesis. *Proceedings of the*
172 *National Academy of Sciences*, 81(14):4586–4590, 1984.
- 173 [10] J. Cudeiro and A. M. Sillito. Looking back: corticothalamic feedback and early visual processing. *Trends*
174 *in neurosciences*, 29(6):298–306, 2006.
- 175 [11] C. Enroth-Cugell and J. G. Robson. The contrast sensitivity of retinal ganglion cells of the cat. *The Journal*
176 *of physiology*, 187(3):517–552, 1966.
- 177 [12] D. Eydin, J. D. Macklis, U. Neubacher, K. Funke, and F. Wörgötter. Selective elimination of corticogenic-
178 ulate feedback abolishes the electroencephalogram dependence of primary visual cortical receptive fields
179 and reduces their spatial specificity. *Journal of Neuroscience*, 23(18):7021–7033, 2003.
- 180 [13] S. Grossberg and E. Mingolla. Neural dynamics of perceptual grouping: Textures, boundaries, and
181 emergent segmentations. In *The adaptive brain II*, pages 143–210. Elsevier, 1987.
- 182 [14] S. Grossberg and J. R. Williamson. A neural model of how horizontal and interlaminar connections of
183 visual cortex develop into adult circuits that carry out perceptual grouping and learning. *Cerebral cortex*,
184 11(1):37–58, 2001.
- 185 [15] E. Harth. Visual perception: A dynamic theory. *Biological Cybernetics*, 22(3):169–180, 1976.
- 186 [16] J. M. Hasse and F. Briggs. Corticogeniculate feedback sharpens the temporal precision and spatial resolution
187 of visual signals in the ferret. *Proceedings of the National Academy of Sciences*, 114(30):E6222–E6230,
188 2017.

- 189 [17] D. H. Hubel and T. N. Wiesel. Receptive fields, binocular interaction and functional architecture in the
190 cat's visual cortex. *The Journal of physiology*, 160(1):106–154, 1962.
- 191 [18] J. F. Jehee and D. H. Ballard. Predictive feedback can account for biphasic responses in the lateral
192 geniculate nucleus. *PLoS computational biology*, 5(5):e1000373, 2009.
- 193 [19] H. E. Jones, I. M. Andolina, B. Ahmed, S. D. Shipp, J. T. Clements, K. L. Grieve, J. Cudeiro, T. E. Salt,
194 and A. M. Sillito. Differential feedback modulation of center and surround mechanisms in parvocellular
195 cells in the visual thalamus. *Journal of Neuroscience*, 32(45):15946–15951, 2012.
- 196 [20] Y. Karklin and E. P. Simoncelli. Efficient coding of natural images with a population of noisy linear-
197 nonlinear neurons. In *Advances in neural information processing systems*, pages 999–1007, 2011.
- 198 [21] Y. Lian, D. B. Grayden, T. Kameneva, H. Meffin, and A. N. Burkitt. Toward a biologically plausible model
199 of lgn-v1 pathways based on efficient coding. *Frontiers in neural circuits*, 13:13, 2019.
- 200 [22] K. McAlonan, J. Cavanaugh, and R. H. Wurtz. Guarding the gateway to cortex with attention in visual
201 thalamus. *Nature*, 456(7220):391–394, 2008.
- 202 [23] J. W. McClurkin, L. M. Optican, and B. J. Richmond. Cortical feedback increases visual information
203 transmitted by monkey parvocellular lateral geniculate nucleus neurons. *Visual neuroscience*, 11(3):601–
204 617, 1994.
- 205 [24] M. H. Mobarhan, G. Halnes, T. Hafting, M. Fyhn, G. T. Einevoll, et al. Firing-rate based network modeling
206 of the dlgn circuit: Effects of cortical feedback on spatiotemporal response properties of relay cells. *PLoS
207 computational biology*, 14(5):e1006156, 2018.
- 208 [25] V. L. Mock, K. L. Luke, J. R. Hembrook-Short, and F. Briggs. Dynamic communication of attention
209 signals between the lgn and v1. *Journal of neurophysiology*, 120(4):1625–1639, 2018.
- 210 [26] B. A. Olshausen and D. J. Field. Natural image statistics and efficient coding. *Network: computation in
211 neural systems*, 7(2):333–339, 1996.
- 212 [27] P. Sastry, S. Shah, S. Singh, and K. Unnikrishnan. Role of feedback in mammalian vision: a new hypothesis
213 and a computational model. *Vision Research*, 39(1):131–148, 1999.
- 214 [28] S. M. Sherman. Tonic and burst firing: dual modes of thalamocortical relay. *Trends in neurosciences*,
215 24(2):122–126, 2001.
- 216 [29] S. M. Sherman and R. Guillery. The role of the thalamus in the flow of information to the cortex.
217 *Philosophical Transactions of the Royal Society of London. Series B: Biological Sciences*, 357(1428):1695–
218 1708, 2002.
- 219 [30] T. Tsumoto, O. Creutzfeldt, and C. Legendy. Functional organization of the corticofugal system from
220 visual cortex to lateral geniculate nucleus in the cat. *Experimental Brain Research*, 32(3):345–364, 1978.
- 221 [31] J. H. Van Hateren and A. van der Schaaf. Independent component filters of natural images compared with
222 simple cells in primary visual cortex. *Proceedings of the Royal Society of London. Series B: Biological
223 Sciences*, 265(1394):359–366, 1998.
- 224 [32] W. Wang, I. M. Andolina, Y. Lu, H. E. Jones, and A. M. Sillito. Focal gain control of thalamic visual
225 receptive fields by layer 6 corticothalamic feedback. *Cerebral cortex*, 28(1):267–280, 2018.
- 226 [33] W. Wang, H. E. Jones, I. M. Andolina, T. E. Salt, and A. M. Sillito. Functional alignment of feedback
227 effects from visual cortex to thalamus. *Nature neuroscience*, 9(10):1330, 2006.

228 **A Appendix**

229 **A.1 Supplementary figures**



(A)

Figure 3: **Block diagram of the model.**

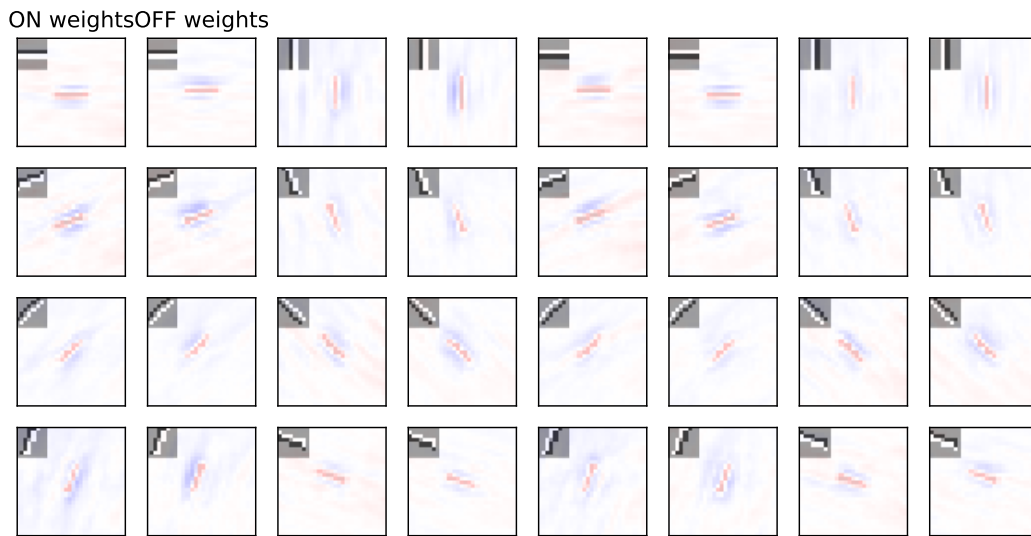


Figure 4: **All the learned feedback weights.** The two sets of weights for all the 16 types of V1 filters, where the V1 filter in LGN space is shown in the upper left corner for reference.